

## Article

# Thermal Performance of Cryogenic Micro-Pin Fin Coolers with Two-Phase Liquid Nitrogen Flows

Kyoung Joon Kim <sup>1,\*</sup>, Hyeon Ho Yang <sup>1</sup>, Wooheon Noh <sup>1</sup>, Bongtae Han <sup>2</sup> and Avram Bar-Cohen <sup>2</sup>

<sup>1</sup> Department of Mechanical Design Engineering, Pukyong National University, Busan 48513, Korea; jkmig12@pukyong.ac.kr (H.H.Y.); suwon4620@pukyong.ac.kr (W.N.)

<sup>2</sup> Department of Mechanical Engineering, University of Maryland, College Park, MD 20742, USA; bthan@umd.edu (B.H.); abc@umd.edu (A.B.-C.)

\* Correspondence: kjkim@pknu.ac.kr; Tel.: +82-51-629-6168

**Abstract:** This study experimentally explores the thermofluidic performance of a cryogenic micro-pin fin cooler with two-phase liquid nitrogen flows. The liquid nitrogen cooling system is introduced to investigate the performance of the micro-pin cooler in a cryogenic condition. The result reveals that the nominal value of the base heat transfer coefficients of the micro-pin fin cooler with liquid nitrogen flows, 240 kW/m<sup>2</sup>-K at a mass flow rate of 2.23 g/s, is an order of magnitude greater than that with FC-72 flows. The result also demonstrates that the base heat transfer coefficient of the micro-pin fin cooler is nearly three times greater than that of the micro-gap cooler, not containing any fins. This study shows the feasibility of the cryogenic micro-pin fin cooler for thermally controlling very high heat density devices such as high-power laser diode bars, of which the heat density can reach 2000 kW/m<sup>2</sup>.

**Keywords:** cryogenic; micro-pin fin; two-phase; liquid nitrogen; heat transfer

check for  
updates

**Citation:** Kim, K.J.; Yang, H.H.; Noh, W.; Han, B.; Bar-Cohen, A. Thermal Performance of Cryogenic Micro-Pin Fin Coolers with Two-Phase Liquid Nitrogen Flows. *Appl. Sci.* **2021**, *11*, 11071. <https://doi.org/10.3390/app112211071>

Academic Editor: Andrea Giachero

Received: 20 October 2021

Accepted: 18 November 2021

Published: 22 November 2021

**Publisher's Note:** MDPI stays neutral with regard to jurisdictional claims in published maps and institutional affiliations.



**Copyright:** © 2021 by the authors. Licensee MDPI, Basel, Switzerland. This article is an open access article distributed under the terms and conditions of the Creative Commons Attribution (CC BY) license (<https://creativecommons.org/licenses/by/4.0/>).

## 1. Introduction

Consistent demand for electronic and photonic devices with high heat density or heat flux, such as microelectronics, power amplifiers, laser diode bars and concentrated photovoltaic cells, necessitates aggressive cooling technologies [1]. Recently, two-phase flows in micro-pin fin arrays have been getting more attention [2–5]. Extensive research has been conducted for single-phase flow in either micro-channels or micro-pin fin arrays [6–9]. Nevertheless, two-phase heat transfer with micro-pin fin arrays is relatively less investigated compared with the single-phase cases.

Krishnamurthy and Peles [10] investigated circular staggered arrays of micro-pin fins with 250 μm height and 100 μm diameter associated with water. It was determined that the nominal value of heat transfer coefficients was 60 kW/m<sup>2</sup>-K. Qu and Siu-Ho [11] investigated the array of 670 μm-high and 200 μm-wide square pin fins with water. They determined that the nominal value of heat transfer coefficients was 70 kW/m<sup>2</sup>-K. McNeil and Raeisi [12] explored in-line arrays of 1000 μm-high and 1000 μm-wide square pin fins with R-113. It was determined that the nominal values of heat transfer coefficients and pressure drops were 3.5 kW/m<sup>2</sup>-K and 3 kPa, respectively. David et al. [13] investigated staggered arrays of 1000 μm-high and 350 μm-wide square pin fins with R-134a. They determined that the nominal value of the base area heat transfer coefficients was 25 kW/m<sup>2</sup>-K. Resser et al. [1] studied in-line and staggered arrays of 305 μm-high square pin fins. The working fluids were deionized water and HFE-7200. The nominal values of base area heat transfer coefficients were 30 kW/m<sup>2</sup>-K for deionized water and 7 kW/m<sup>2</sup>-K for HFE-7200, respectively. The nominal values of pressure drops were 35 kPa for deionized water and 30 kPa for HFE-7200, respectively.

Cryogenic cooling could be a more effective solution for the performance and reliability of devices with an extreme heat density such as LD bars. Zhang et al. [14] investigated

the flow boiling mechanism through micro-tubes with liquid nitrogen. The explored tube diameters were 0.531, 0.834, 1.042 and 1.931 mm. It was claimed that nucleate boiling for the low mass quality region and convection evaporation for the high mass quality region govern heat transfer. Their study results found the critical heat flux (CHF) with micro-tubes to be higher compared with classical channels and the CHF increased with the mass flux. Chen et al. [15] explored heat transfer mechanisms of boiling liquid nitrogen flow through a horizontal tube. The internal diameter of the tube was 1.98 mm. They proposed a correlation considering the effects of convective evaporation and nucleate boiling to predict heat transfer coefficients in the channel. To the best of our knowledge, only one piece of research [16] has been reported for cryogenic cooling with micro-pin fin arrays, though research on cryogenic cooling in micro- or mini-tubes, as mentioned, has been consistently conducted.

This paper extends the preceding literature [16] focusing on thermofluidic characteristics of cryogenic LN<sub>2</sub> flow in micro-coolers. This paper begins by introducing and discussing correlations predicting the heat transfer and pressure drop in micro-pin fin arrays with a two-phase flow. Then, the paper discusses the experimental apparatus and procedure for exploring the thermofluidic performance of the cryogenic micro-pin fin cooler with LN<sub>2</sub> flow. Finally, this paper discusses the thermofluidic performance of the cryogenic micro-pin fin cooler, compares the performance between the cryogenic micro-pin fin cooler and the cryogenic micro-gap cooler and explores the effect of the refrigerant by comparing the performance between the cryogenic micro-pin fin cooler with an LN<sub>2</sub> flow and the micro-pin fin cooler with an FC-72 flow.

## 2. Correlations

There are several correlations [1,10,11] available to predict the thermofluidic performance of a micro-pin fin array with a two-phase flow. In this study, correlations developed or utilized by Krishnamurthy and Peles [10] were employed because the fin diameter, fin height and fin pitch of their micro-pin fin array were quite similar to those of the micro-pin fin cooler in this investigation. Neither development of new correlations nor evaluation of utilized correlations were the primary objectives of this study. The correlations were only employed to generate auxiliary data associated with FC-72 flows.

### 2.1. Heat Transfer

Peles [10] used correlations, based on a Chen-type model, to evaluate heat transfer coefficients. Chen [17] defined a heat transfer coefficient for two-phase state,  $h_{tp}$ , for forced convective boiling in a tube as:

$$h_{tp} = F \cdot h_{sp} + S \cdot h_{nb} \quad (1)$$

where  $F$  denotes an enhancement factor,  $h_{sp}$  denotes a heat transfer coefficient for the single-phase state,  $S$  denotes a suppression factor and  $h_{nb}$  denotes a heat transfer coefficient for nucleate boiling.

$F$  is defined as the ratio of the two-phase Reynolds number to the liquid Reynolds number and  $S$  is defined as the ratio of the effective superheat to the total superheat of the wall. The decrease of  $S$  denotes the decrease of the effective superheat, and eventually induces the suppression of the nucleate boiling.

Peles [10] found that convective boiling is the dominant heat transfer mechanism, and thus the nucleate boiling term in Equation (1) is neglected.

$h_{tp}$  is re-expressed as:

$$h_{tp} = F h_{sp} \quad (2)$$

For a case where  $Pr \approx 1$ ,  $F$  is defined as in [10]:

$$F = \left( \phi_l^2 \right)^{0.2475} \quad (3)$$

For a case where  $Pr \neq 1$ , Equation (3) is multiplied by  $Pr^{0.333}$  by using the method adopted by Bennett et al. [18], as shown below:

$$F = \left(\phi_l^2\right)^{0.2475} Pr^{0.333} \tag{4}$$

where  $\phi_l$  is a two-phase frictional multiplier.

Similar to Zhang and Hibiki [19]’s method, an adjustment parameter  $\zeta$  is considered, and  $F$  is rewritten as:

$$F = \zeta \left(\phi_l^2\right)^{0.2475} Pr^{0.333} \tag{5}$$

Consequently, the two-phase heat transfer coefficient is written as:

$$h_{tp} = \zeta \left(\phi_l^2\right)^{0.2475} Pr^{0.333} h_{sp} \tag{6}$$

The value of the adjustment parameter,  $\zeta$ , is 1.4. [20].

A two-phase friction multiplier  $\phi_l$  is determined using the correlation proposed by Chisholm and Laird [21], as:

$$\left(\phi_l\right)^2 = \frac{\left(\Delta P_f\right)_{tp}}{\left(\Delta P_f\right)_f} = 1 + \frac{C}{X_{vv}} + \frac{1}{X_{vv}^2} \tag{7}$$

where  $C = 0.24$  is an empirically defined constant.  $X_{vv}$  is the Martinelli parameter [22], defined as:

$$X_{vv} = \left[ \frac{\left(\Delta P_f / \Delta Z\right)_f}{\left(\Delta P_f / \Delta Z\right)_v} \right]^{\frac{1}{2}} \tag{8}$$

$$\left(\Delta P_f\right)_f = \frac{fN(G(1-x))^2}{2\rho_f} \tag{9}$$

$$\left(\Delta P_f\right)_v = \frac{fN(Gx)^2}{2\rho_v} \tag{10}$$

where  $(\Delta P_f / \Delta Z)_f$  is the frictional pressure gradient assuming only liquid flows through the channel,  $(\Delta P_f / \Delta Z)_v$  is the frictional pressure gradient assuming only vapor flows through the channel,  $f$  is the Blasius type friction factor,  $N$  is number of fin rows,  $G$  is the mass flux,  $x$  is the quality,  $\rho_f$  is the liquid density and  $\rho_v$  is the vapor density.

$f$  is defined as [23]:

$$f = 63.246(Re_d)^{-0.7797} \tag{11}$$

where  $Re_d$  is the Reynolds number ( $Re_d = Gd_e / \mu$ ),  $d_e$  is the equivalent diameter of a square micro-pin fin and  $\mu$  is dynamic viscosity.

In Equation (11), the correlation was developed to predict the experimental results within 5% [23].

In Equation (6), the single-phase heat transfer coefficient term  $h_{sp}$  is defined as:

$$h_{sp} = \frac{Nu \cdot k_f}{d_e} \tag{12}$$

where  $Nu$  is the Nusselt number,  $k_f$  is the thermal conductivity of fluid and  $d_e$  is the equivalent diameter of a fin.

To evaluate  $Nu$ , the correlation by Short et al. [24] was utilized, defined as:

$$Nu = 0.76 \left(\frac{St}{d_e}\right)^{0.16} \left(\frac{St_l}{d_e}\right)^{0.2} \left(\frac{H_{fin}}{d_e}\right)^{-0.11} Re^{0.33} \tag{13}$$

where  $S_t$ ,  $S_l$  and  $H_{fin}$  are transverse fin spacing, longitudinal fin spacing and fin height, respectively.

## 2.2. Pressure Drop

The local two-phase pressure drop  $\Delta P_{tp}(x)$  is determined using the equation below [10]:

$$\Delta P_{tp}(x) = \frac{1}{x - x_i} \int_{x_i}^x \phi_l^2 (\Delta P_f)_f dx + \Delta P_{accl} \quad (14)$$

The acceleration pressure drop,  $\Delta P_{accl}$  is evaluated as [10]:

$$\Delta P_{accl} = \left\{ \frac{G^2 x^2}{\rho_g \alpha} + \frac{G^2 (1-x)^2}{\rho_l (1-\alpha)} \right\}_{outlet} - \left\{ \frac{G^2 x^2}{\rho_g \alpha} + \frac{G^2 (1-x)^2}{\rho_l (1-\alpha)} \right\}_{inlet} \quad (15)$$

$$\alpha_h = \frac{x v_g}{(1-x)v_l + x v_g} \quad (16)$$

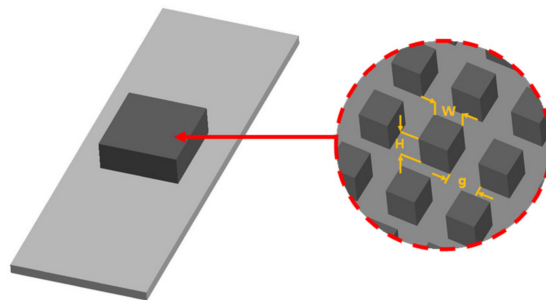
$$\frac{\alpha}{\alpha_h} = 1 + 0.04503(f)^{0.34} \ln(x) \quad (17)$$

where  $\alpha$  is the void fraction,  $\alpha_h$  is the homogenous void fraction,  $\rho_g$  is the gas density,  $\rho_l$  is the liquid density,  $v_g$  is the gas specific volume,  $v_l$  is the liquid specific volume and  $f$  is the liquid friction factor.

## 3. Experimental Apparatus and Procedure

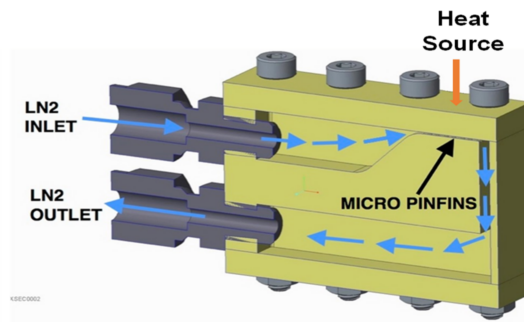
This section visualizes the physical structure of the copper micro-pin fin array. Then, the discussion of the cryogenic micro-pin fin cooler follows. The test rig of the micro-pin fin cooler and the experimental procedure are explained in the following subsection.

The physical structure of the copper micro-pin fin array is illustrated in Figure 1. The fin width is 150  $\mu\text{m}$ , the fin heights are 100, 300 and 500  $\mu\text{m}$  and the gap between adjacent fins is 150  $\mu\text{m}$ . The number of fins is 1600, and the base area of the array is 12 mm  $\times$  12 mm.



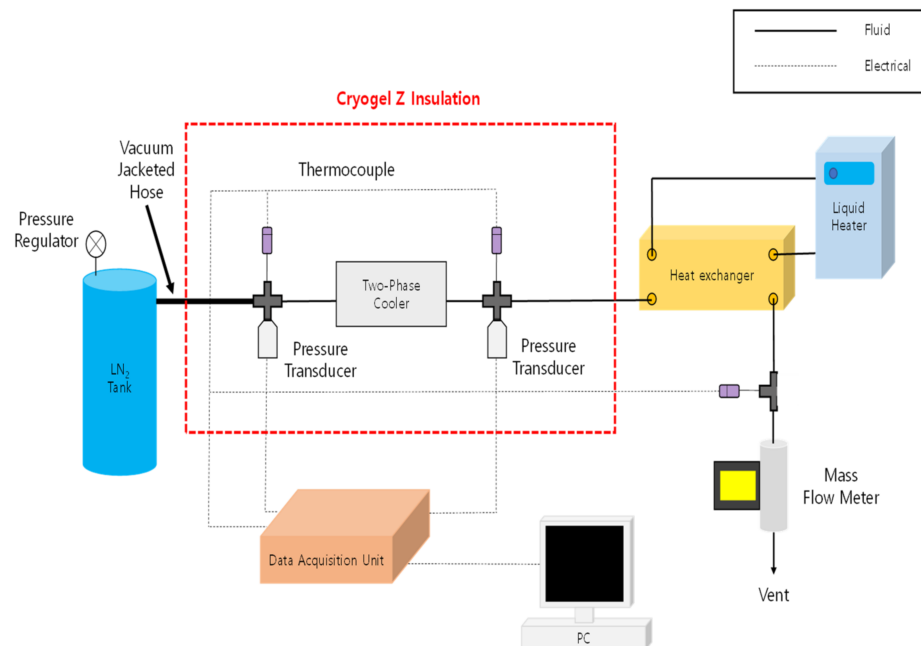
**Figure 1.** Structure of the copper micro-pin fin array.

The physical structure of the cryogenic micro-pin fin cooler is visualized by showing its cross-sectional view, as presented in Figure 2. A manifold, upper and lower plates and an embedded micro-pin fin array compose the cooler. The base material is copper. The manifold is 55.1 mm long, 24.9 mm wide and 30 mm high. For micro-pin fin arrays, available references [16] show the fin width ranging from 100 to 350  $\mu\text{m}$  and the fin pitch from 150 to 431  $\mu\text{m}$ . To obtain high base heat transfer coefficients at reasonable pressure drops, the dimensions of micro-pin fins were selected by considering the values of the references and fabrication capability. The selected values were a width of 150  $\mu\text{m}$ , height of 300  $\mu\text{m}$  and pitch of 300  $\mu\text{m}$ . The base area of the array was 10 mm  $\times$  10 mm. The working fluid was  $\text{LN}_2$ , and a heat source, i.e., a hot device, was placed on the top of the cooler.



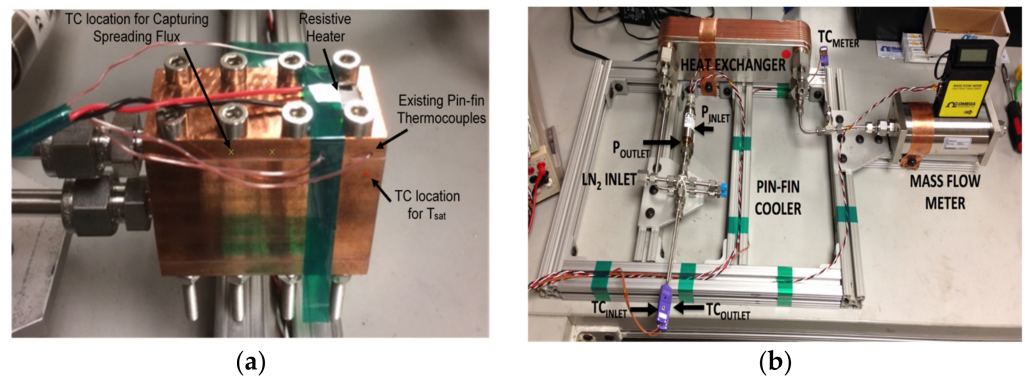
**Figure 2.** Cross-section of the cryogenic micro-pin fin cooler.

Figure 3 illustrates a test rig to investigate the thermofluidic performance of a cryogenic microcooler with a two-phase LN<sub>2</sub> flow. LN<sub>2</sub> flow is controlled by a pressure regulator, and LN<sub>2</sub> is transported through the microcooler. In the microcooler, the heat is absorbed from the hot device. Consequently, the liquid phase changes to the vapor phase. The heat exchanger is used to evaporate the excess of LN<sub>2</sub>, and then LN<sub>2</sub> is heated by a water loop maintained at 25 °C. The test rig utilizes omega E-type thermocouples measuring temperature and cryogenic pressure transducers measuring pressure at the first and the second four-way junctions. The test rig also uses a mass flow meter to monitor the mass flow rate and 316SS for compression fittings and tubing. The flow loop apparatus is insulated with cryogel Z insulation. The measured data are acquired by LabVIEW with an NI 9214 module for temperature and an NI9205 module for voltage.



**Figure 3.** Schematic of a test rig to investigate the performance of cryogenic microcoolers with LN<sub>2</sub> flows.

Figure 4a,b provides actual images of the micro-pin fin cooler manifold and the assembled LN<sub>2</sub> flow loop apparatus. The thermocouple location and the placement of the resistive heater of the micro-pin fin cooler manifold are shown in Figure 4a. This study also explores the performance of the micro-gap cooler. Its performance is employed as an analysis baseline. The micro-gap cooler, containing an un-finned micro-gap, is structurally quite similar to the micro-pin fin cooler despite having no micro-pin fin. Both the measurement and operating conditions for the micro-gap cooler and the micro-pin fin cooler are very similar.



**Figure 4.** (a) Micro-pin fin cooler manifold; (b) Assembled LN<sub>2</sub> flow loop apparatus.

Nominal values of measurement accuracy and uncertainty need to be mentioned to assure measurement reliability. The nominal accuracy values are 0.3% for the cryogenic pressure transducer, 1% for the nitrogen mass flow meter, 0.2% for the power supply and  $\pm 0.5$  °C for the thermocouple. In this study, measurements were repeated two or three times for each mass flow rate. The uncertainty in exit quality was estimated using the method shown in [1], and the estimated typical uncertainty was 3.2%. The measured data should be reliable considering such reasonable values of accuracy and uncertainty.

#### 4. Results and Discussion

In this section, the thermofluidic performance of the cryogenic micro-pin fin cooler is discussed. Then, it is compared with that of the cryogenic micro-gap cooler. In the following analysis, the thermofluidic performance of the cryogenic micro-pin fin cooler with LN<sub>2</sub> will be compared with the performance, either measured or predicted using correlations, of the micro-pin fin cooler with FC-72.

Figure 5a,b shows the base heat transfer coefficient and pressure drop of the cryogenic micro-pin fin cooler, associated with LN<sub>2</sub> flow, as a function of exit quality. The exit quality values range from 7.5 to 30%. All the results shown in Figure 5a,b were obtained using the test rig shown in Figure 4a,b. The applied chip heater powers were 30, 70 and 96 W.

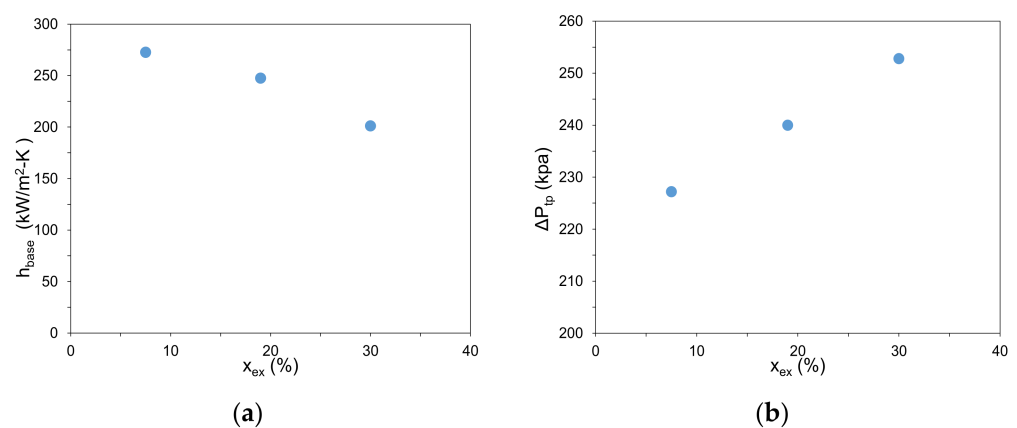


**Figure 5.** (a) Base heat transfer coefficient and (b) pressure drop of the cryogenic micro-pin fin cooler as a function of exit quality.

$h_{base}$  denotes a base heat transfer coefficient, defined as  $q/[A(T_s - T_{inf})]$ .  $q$  is the heat transfer rate,  $A$  is the base area,  $T_s$  is the surface temperature and  $T_{inf}$  is the fluid temperature. The result shows the decrease of  $h_{base}$  values ranging from 273 to 201 kW/m<sup>2</sup>-K and the increase of pressure drop values ranging from 227 to 253 kPa as the exit quality increases. This reduction of the  $h_{base}$  value with the increase of the exit quality value might

be explained by the decrease of the mass flow rate as the power dissipation and vapor fraction increase.

Figure 6a,b shows the base heat transfer coefficient and the pressure drop of the cryogenic micro-gap cooler, associated with two mass flux values of LN<sub>2</sub> flow, as a function of exit quality. The results show  $h_{\text{base}}$  values ranging from 92 to 103 kW/m<sup>2</sup>-K and  $\Delta P_{\text{tp}}$  values ranging from 55 to 69 kPa associated with a mass flux of 3.2 g/s, and  $h_{\text{base}}$  values ranging from 85 to 89 kW/m<sup>2</sup>-K and  $\Delta P_{\text{tp}}$  values ranging from 39 to 48 kPa associated with a mass flux of 2.3 g/s. Both greater  $h_{\text{base}}$  and  $\Delta P_{\text{tp}}$  values with a greater mass flux imply conflicting aspects, i.e., affirmative and negative effects, of the increase of the mass flux. It should be noted that the value and range of the exit quality used for Figure 6a,b are considerably smaller than those for Figure 5a,b.

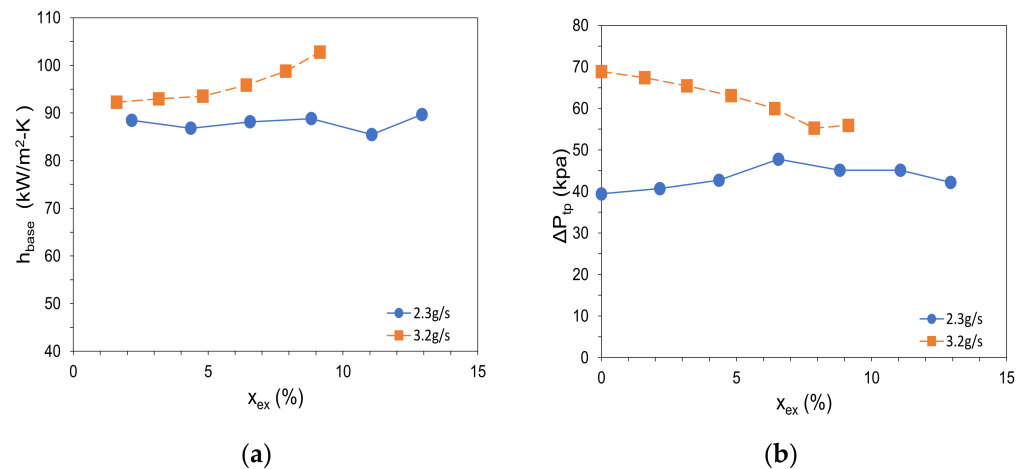


**Figure 6.** (a) Base heat transfer coefficient and (b) pressure drop of the cryogenic micro-gap cooler as a function of exit quality.

FC-72 is one of the widely utilized fluids for the research of two-phase flow heat transfer with mini or micro-channels. In this study, the micro-pin fin array with FC-72 flow was used as a baseline to evaluate the thermofluidic performance of the LN<sub>2</sub> micro-pin fin cooler. Prior to a detailed discussion regarding the thermofluidic performance with two fluids, it is useful to discuss the thermofluidic properties of N<sub>2</sub> and FC-72, as shown in Table 1.

**Table 1.** Descriptions of N<sub>2</sub> and FC-72's properties [25–28].

Property	Unit	N <sub>2</sub>	FC-72
Molecular weight		28	338
Boiling temperature	K	77.3	329.1
	°C	−195.9	56
Liquid enthalpy	kJ/kg	−122.1	59.8
Latent heat of vaporization	kJ/kg	198.8	84.7
Vapor enthalpy	kJ/kg	76.7	144.5
Liquid density	kg/m <sup>3</sup>	806	1680
Vapor density	kg/m <sup>3</sup>	4.6	13
Kinematic viscosity of liquid	10 <sup>6</sup> m <sup>2</sup> /s	0.19	0.38
Liquid specific heat	kJ/kg-K	2.041	1.1
Liquid thermal conductivity	W/m-K	0.135	0.057
Thermal diffusivity	10 <sup>6</sup> m <sup>2</sup> /s	0.082	0.031

Table 1 shows that N<sub>2</sub> has about a 252-K lower boiling temperature, nearly twice the latent heat of vaporization, nearly twice the liquid specific heat, 2.4 times larger thermal conductivity, about half the kinematic viscosity and 2.6 times greater thermal diffusivity

compared with FC-72. The comparison of crucial thermofluidic properties implies that  $N_2$  might be better than FC-72 for heat transfer enhancement in both sensible and latent heat transfer modes.

Figures 7 and 8 present the base heat transfer coefficient,  $h_{base}$ , and the pressure drop,  $\Delta P_{tp}$ , of the cryogenic micro-pin fin and micro gap coolers. Both  $h_{base}$  and  $\Delta P_{tp}$  values are shown with various exit quality values for various mass flux values of  $LN_2$  and FC-72. In Figures 7 and 8, fin, gap, value of g/s and value of  $\mu m$  denote a micro-pin fin cooler, micro-gap cooler, mass flux and fin height, respectively.

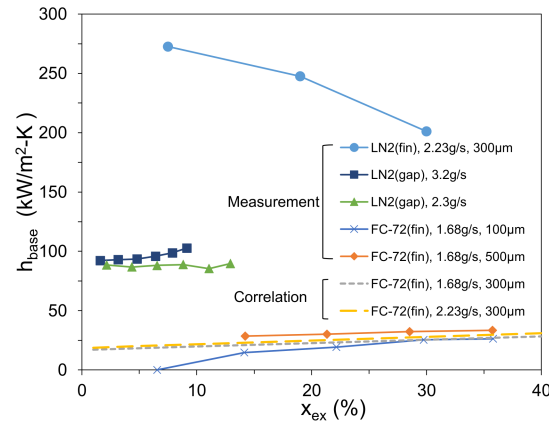


Figure 7. Base heat transfer coefficient of the cryogenic micro-pin fin and micro-gap coolers as a function of exit quality for various mass fluxes of  $LN_2$  and FC-72.

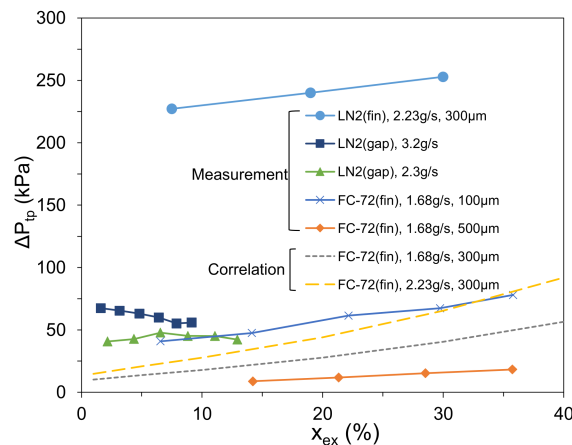


Figure 8. Pressure drop of the cryogenic micro-pin fin and micro-gap coolers as a function of exit quality for various mass fluxes of  $LN_2$  and FC-72.

The analysis of FC-72 is either based on measured or correlation-evaluated results. The correlations shown in Equations (6)–(17) were used to evaluate  $h_{base}$  and  $\Delta P_{tp}$  values for similar fin height and mass flux conditions compared to the  $LN_2$  micro-pin fin cooler.

Figure 7 reveals that the nominal value of  $h_{base}$  of the micro-pin fin cooler with  $LN_2$  flow is nearly an order of magnitude greater than that of the micro-pin fin cooler with FC-72 flow, showing the average value with  $LN_2$  of  $240 \text{ kW/m}^2\text{-K}$  and that with FC-72 of  $23 \text{ kW/m}^2\text{-K}$ . In this comparison, the mass flux and fin height are  $2.23 \text{ g/s}$  and  $300 \mu m$ , respectively. The superior thermofluidic properties of  $LN_2$  may explain this interesting result.

Figure 7 shows the average  $h_{base}$  value of the micro-gap cooler with  $LN_2$  flow is  $78 \text{ kW/m}^2\text{-K}$  at a mass flux of  $2.23 \text{ g/s}$  and fin height of  $300 \mu m$ . This result demonstrates that the  $h_{base}$  value with the micro-pin fin cooler could be about three times greater than that with the micro-gap cooler. The effect of surface area enhancement by the micro-fin

array can explain the considerably better heat transfer performance with the micro-pin fin cooler.

The trend of the  $h_{\text{base}}$  of the micro-pin fin cooler can be seen to differ from that of the micro-gap cooler. The difference of the two-phase heat transfer behavior with the exit quality between the micro-pin fin cooler and the micro-gap cooler might be explained by the nearly three times greater exit quality associated with the micro-pin fin cooler, in terms of average quality value, than that with the micro-gap cooler.

The result shown in Figure 7 visualizes the feasibility of the cryogenic micro-pin fin cooler when thermally managing very high heat density devices such as high power laser diode (LD) bars [16], of which the heat density can reach  $2000 \text{ kW/m}^2$ . For example, the cryogenic micro-pin fin cooler may control such a high power laser diode bar at an excess temperature, i.e., the temperature difference between the LD bar and the  $\text{LN}_2$  flow, of about 10 K.

Figure 8 shows that  $\Delta P_{\text{tp}}$  values of the micro-pin fin cooler increase as the exit quality for both  $\text{LN}_2$  and FC-72 flows increases. The pressure drop is fundamentally affected by various physical parameters including local quality, fluid velocity, characteristic length, viscosity and density. Although explaining the pressure drop behavior for either  $\text{LN}_2$  or FC-72 flow is quite challenging due to the complicated mechanism of interrelated effects of aforementioned parameters, increasing momentum dissipation induced by the increase of the vapor fraction may explain such an increase of  $\Delta P_{\text{tp}}$  values.

Figure 8 shows that the values of  $\Delta P_{\text{tp}}$  with  $\text{LN}_2$  are greater than those with FC-72. It can also be seen that the values of  $\Delta P_{\text{tp}}$  with the micro-pin fin cooler are greater than those with the micro gap cooler. The effect of the micro-pin fin array on the pressure drop along the microcooler should be understood for better design of the micro-pin fin cooler. Hence, physical aspects of the considerably greater values of  $\Delta P_{\text{tp}}$  with the micro-pin fin cooler compared with the micro gap cooler should be rigorously investigated, employing sophisticated measurement tools, in a future study.

In Figures 7 and 8, the correlation prediction can be seen to roughly agree with the measurement. This discrepancy might be explained by the difference of fin heights and flow rates between the measurement and prediction, the characteristics of correlations fundamentally developed using water data and the very complicated physical behavior of  $\text{LN}_2$  flow through the micro-pin fin cooler. As previously mentioned, it should be noted that the evaluation of the correlations was not a primary objective of this study. The correlations [10] were utilized to provide supplementary data associated with FC-72 flows and to check the general trends of the measurement data.

## 5. Conclusions

This study aimed to investigate the thermofluidic performance of a cryogenic micro-pin fin cooler with an  $\text{LN}_2$  flow. The experimental apparatus was implemented for measurement. Heat transfer coefficient and pressure drop values were carefully measured. Supplementary results of the heat transfer coefficient and pressure drop with FC-72 flows were generated, employing correlations utilized from the literature. The surface area effect of the micro-pin fin array on the thermofluidic performance was explored by comparing the micro-pin fin cooler with the micro-gap cooler. The refrigerant effect on the thermofluidic performance of the micro-pin fin cooler was also explored by comparing the case with the  $\text{LN}_2$  flow to the case with the FC-72 flow.

Several interesting results were found in this study. First, the study revealed that the nominal value of the base heat transfer coefficient,  $h_{\text{base}}$ , of the micro-pin fin cooler with an  $\text{LN}_2$  flow was  $250 \text{ kW/m}^2\text{-K}$  at a mass flow rate of  $2.23 \text{ g/s}$ , which was an order of magnitude greater than that with a FC-72 flow. This interesting result might be explained by superior thermofluidic properties of  $\text{LN}_2$  when compared with FC-72. Second, the study result demonstrated that the  $h_{\text{base}}$  value with the micro-pin fin cooler could be about three times greater than that with the micro-gap cooler. This was mainly due to the affirmative effect of the surface area enhancement by the micro-fin array. Third, the result revealed

the potential capability of the cryogenic micro-pin fin cooler to thermally manage very high heat density devices, e.g., high power laser diode bars, of which the heat density can reach  $2000 \text{ kW/m}^2$ . Last, the results found that the pressure drop,  $\Delta P_{tp}$ , values of the micro-pin fin cooler increased with increases of the exit quality for both  $\text{LN}_2$  and FC-72 flows. The increase of the vapor fraction caused an increase of momentum dissipation. This mechanism may explain such an increase of  $\Delta P_{tp}$  values.

**Author Contributions:** Conceptualization, K.J.K., B.H. and A.B.-C.; methodology, K.J.K.; software, H.H.Y.; validation, H.H.Y. and W.N.; formal analysis, H.H.Y.; investigation, W.N.; resources, B.H. and A.B.-C.; data curation, K.J.K. and H.H.Y.; writing—original draft preparation, K.J.K.; writing—review and editing, K.J.K.; visualization, H.H.Y.; supervision, K.J.K., B.H. and A.B.-C.; project administration, K.J.K., B.H. and A.B.-C.; funding acquisition, K.J.K., All authors have read and agreed to the published version of the manuscript.

**Funding:** This work was supported by the National Research Foundation of Korea (NRF) grant funded by the Korea government (MSIT) (No. 2019R1F1A1061585).

**Institutional Review Board Statement:** Not applicable.

**Informed Consent Statement:** Not applicable.

**Data Availability Statement:** Data are contained within the article.

**Conflicts of Interest:** The authors declare no conflict of interest.

## Nomenclature

$A$	base area [ $\text{m}^2$ ]
$C$	constant in Equation (7)
$d_e$	equivalent diameter of a fin [m]
$F$	enhancement factor
$f$	friction factor
$G$	mass flux [ $\text{kg/m}^2\text{s}$ ]
$H_{fin}$	fin height [m]
$h$	heat transfer coefficient [ $\text{W/m}^2\text{-k}$ ]
$h_{base}$	base heat transfer coefficient [ $\text{W/m}^2\text{-k}$ ]
$k$	thermal conductivity [ $\text{W/m-k}$ ]
$N$	number of fin rows in longitudinal direction
$Nu$	Nusselt number
$Pr$	Prandtl number
$\Delta P$	pressure drop [Pa]
$\Delta P_f$	pressure drop due to friction [Pa]
$\Delta P_{accl}$	pressure drop due to acceleration [Pa]
$q$	heat transfer rate [W]
$Re$	Reynolds number
$S$	suppression factor
$S_t$	transverse fin spacing [m]
$S_L$	longitudinal fin spacing [m]
$T_{inf}$	fluid temperature [ $^\circ\text{C}$ ]
$T_s$	surface temperature [ $^\circ\text{C}$ ]
$X$	Martinelli parameter
$x$	quality
Greek symbols	
$\alpha$	void fraction
$\rho$	density [ $\text{kg/m}^3$ ]
$\mu$	dynamic viscosity [ $\text{Pa}\cdot\text{s}$ ]
$\nu$	specific volume [ $\text{m}^3/\text{kg}$ ]
$\phi_l$	two-phase frictional multiplier
$\zeta$	adjustment parameter

## Subscripts

d	diameter
f	fluid
g	gas
h	homogenous flow model
l	liquid
nb	nucleate boiling
sp	single-phase
tp	two-phase
v	vapor
vv	viscous-viscous

## References

1. Reeser, A.; Bar-Cohen, A.; Hetsroni, G. High quality flow boiling heat transfer and pressure drop in microgap pin fin array. *Int. J. Heat Mass Transf.* **2014**, *78*, 974–985. [[CrossRef](#)]
2. Lingjian, K.; Zhigang, L.; Lei, J.; Mingming, L.; Ying, L. Experimental study on flow and heat transfer characteristics at onset of nucleate boiling in micro pin fin heat sinks. *Exp. Therm. Fluid Sci.* **2020**, *115*, 109946. [[CrossRef](#)]
3. Chien, L.H.; Cheng, Y.T.; Lai, Y.T.; Yan, W.M.; Ghalambaz, M. Experimental and numerical study on convective boiling in a staggered array of micro pin-fin microgap. *Int. J. Heat Mass Transf.* **2020**, *149*, 119203. [[CrossRef](#)]
4. Yin, L.; Jiang, P.; Xu, R.; Hu, H. Water flow boiling in a partially modified microgap with shortened micro pin fins. *Int. J. Heat Mass Transf.* **2020**, *155*, 119819. [[CrossRef](#)]
5. Jung, K.M.; Krishnan, R.A.; Kumar, U.G.; Lee, H.J. Experimental study on two-phase pressure drop and flow boiling heat transfer in a micro pin fin channel heat sink under constant heat flux. *Exp. Heat. Trans.* **2021**, *34*, 162–185. [[CrossRef](#)]
6. Gorasiya, A.; Saha, S.K. Single phase laminar fluid flow and heat transfer in microchannel with cylindrical and parallelepiped micro-fins. *Heat. Mass. Transf.* **2019**, *55*, 613–626. [[CrossRef](#)]
7. Kewalramani, G.V.; Hedau, G.; Saha, S.K.; Agrawal, A. Study of laminar single phase frictional factor and Nusselt number in In-line micro pin-fin heat sink for electronic cooling applications. *Int. J. Heat Mass Transf.* **2019**, *138*, 796–808. [[CrossRef](#)]
8. Kong, D.; Jung, K.W.; Jung, S.; Jung, D.; Schaadt, J.; Iyengar, M.; Malone, C.; Kharangate, C.R.; Asheghi, M.; Goodson, K.E.; et al. Single-phase thermal and hydraulic performance of embedded silicon micro-pin fin heat sinks using R245fa. *Int. J. Heat Mass Transf.* **2019**, *141*, 145–155. [[CrossRef](#)]
9. Yang, M.; Li, M.T.; Hua, Y.C.; Wang, W.; Cao, B.Y. Experimental study on single-phase hybrid microchannel cooling using HFE-7100 for Liquid-cooled chips. *Int. J. Heat Mass Transf.* **2020**, *160*, 120230. [[CrossRef](#)]
10. Krishnamurthy, S.; Peles, Y. Flow boiling of water in a circular staggered micro-pin fin heat sink. *Int. J. Heat Mass Transf.* **2008**, *51*, 1349–1364. [[CrossRef](#)]
11. Qu, W.; Siu-Ho, A.M. Experimental study of saturated flow boiling heat transfer in an array of staggered micro-pin fins. *Int. J. Heat Mass Transf.* **2009**, *52*, 1853–1863. [[CrossRef](#)]
12. McNeil, D.A.; Raeisi, A.H.; Kew, P.A.; Bobbili, P.R. A comparison of flow boiling heat-transfer in in-line mini pin fin and plane channel flows. *Appl. Therm. Eng.* **2010**, *30*, 2412–2425. [[CrossRef](#)]
13. David, T.; Mendler, D.; Mosyak, A.; Bar-Cohen, A.; Hestroni, G. Thermal management of time-varying high heat flux electronic devices. *ASME J. Electron. Packag.* **2014**, *136*, 021003. [[CrossRef](#)]
14. Qi, S.L.; Zhang, P.; Wang, R.Z.; Xu, L.X. Flow boiling of liquid nitrogen in micro-tubes: Part II—Heat transfer characteristics and critical heat flux. *Int. J. Heat Mass Transf.* **2007**, *50*, 5017–5030. [[CrossRef](#)]
15. Chen, S.; Chen, X.; Chen, L.; Zhang, Q.; Hou, Y. Experimental study on the heat transfer characteristics of saturated liquid nitrogen flow boiling in small-diameter horizontal tubes. *Exp. Therm. Fluid Sci.* **2019**, *101*, 27–36. [[CrossRef](#)]
16. Kim, K.J.; Han, B.; Bar-Cohen, A. Thermal and optical performance of cryogenically cooled laser diode bars mounted on pin-finned microcoolers. *Appl. Phys. B* **2021**, *127*, 43. [[CrossRef](#)]
17. Chen, J.C. Correlation for boiling heat transfer to saturated fluids in convective flow. *Ind. Eng. Chem. Proc. Des. Dev.* **1966**, *5*, 322–329. [[CrossRef](#)]
18. Bennett, L.; Chen, J. Forced convective boiling in vertical tubes for saturated components and binary mixtures. *J. Am. Inst. Chem. Eng.* **1980**, *26*, 454–461. [[CrossRef](#)]
19. Zhang, W.; Hibiki, T.; Mishima, K. Correlation for flow boiling heat transfer at low liquid Reynolds number in small diameter channels. *ASME J. Heat Transf.* **2005**, *127*, 1214–1221. [[CrossRef](#)]
20. Krishnamurthy, S.; Peles, Y. Gas-liquid two-phase flow across a bank of micropillars. *Phys. Fluids* **2007**, *19*, 043302. [[CrossRef](#)]
21. Chisholm, D.; Laird, A.D.K. Two-phase flow in rough tubes. *Trans. ASME* **1958**, *80*, 276–286.
22. Lockhart, R.W.; Martinelli, R.C. Proposed correlation of data for isothermal two-phase, two-component flow in pipes. *Chem. Eng. Prog.* **1949**, *45*, 39–48.
23. Koşar, A.; Peles, Y. Thermal-hydraulic performance of MEMS based pin fin heat sink. *ASME J. Heat Transf.* **2006**, *128*, 121–131. [[CrossRef](#)]

- 
24. Short, B.E.; Raad, P.E.; Price, D.C. Performance of pin fin cast aluminum, coldwalls, part 2: Colburn j-factor correlations. *J. Thermophys. Heat Transf.* **2002**, *16*, 397–403. [[CrossRef](#)]
  25. Hands, B.A. *Cryogenic Engineering*, 1st ed.; Academic Press: Niwot, CO, USA, 1986.
  26. Haynes, W.M. *CRC Chemistry/Physics Handbook*, 93rd ed.; CRC Press: New York, NY, USA, 2013.
  27. 3M Fluorinert. Product Information. 2000.
  28. Mudawar, I.; Anderson, T.M. Parametric Investigation into the effects of pressure, subcooling, surface augmentation and choice of coolant on pool boiling in the design of cooling systems for high-power-density electronic chips. *ASME J. Electron. Packag.* **1990**, *112*, 375–382. [[CrossRef](#)]